A Non-Destructive Investigation of Plutonium Reference Items Used for Calibration - 8385

D. Curtis, M. Wormald, C.G. Wilkins
Canberra UK Ltd.
Harwell, Didcot, Oxfordshire, OX11 0TA, UK

S. Croft
Canberra Industries Inc.
800 Research Parkway, Meriden, CT 06450, USA

ABSTRACT

The calibration of Non-Destructive Assay (NDA) equipment relies on the availability of certified items of known content and construction. Increasing use is being made of calculational tools to create calibration data and so representative standards are no longer always needed. However, even with this approach it is invaluable to benchmark the tools against the measured response under well known conditions and to apply the Measured: Calculated ratio as a scaling factor. Reference sources for Pu are typically doubly encapsulated for safety reasons and contain Pu of well known chemical form, elemental composition, relative isotopic composition and mass. Destructive analysis techniques are used to characterize the materials and so these attributes are usually known with far greater accuracy than that achievable by the NDA methods to which they are being applied. Construction details are also usually provided in order to permit attenuation and related factors to be estimated.

This work concerns the empirical investigation of a set of encapsulated PuO_2 powder standards. The characterization and fabrication of the items is adequately documented with the exception of fill height. The fill height governs the powder density and in turn both the self attenuation of photons and the self multiplication of neutrons, consequently this is an important omission. Initially the location and dimensions of the internal plunger cup was used as a basis to estimate the packing density, but later records of plunger positions made at the time of filling were found and significant revisions followed. As a consequence of discrepancies observed in measurements designed to evaluate a new lump correction algorithm we were led to investigate the powder density and distribution directly by gamma-ray scanning. In some cases this resulted in revised density estimates. Equally importantly it was discovered that for the smallest mass items, the powder was not held fixed in the form of a uniform disc by the spring loaded plunger but rather could flow inside the inner capsule. In this paper we describe the nature of the investigation, report the salient findings and explain the implications for modeling the sources for the calibration of NDA equipment.

INTRODUCTION

The valid characterization and calibration of nondestructive assay instrumentation ultimately relies on the quality of the reference items available for measurement. At Canberra UK, we make use of a Pu/Ga 'bead', certified Pu/Ga disks [1] and certified double walled cylindrical canisters of reactor grade (RG) PuO_2 [2]. Knowledge of the chemical form, purity and construction are needed in order to correct observed data for various effects. In the case of gamma-ray calibration the most important effect would be that of self attenuation and attenuation by the encapsulation [3-5]. For low energy lines only the surface of the nuclear material is visible and the geometry of the item is key information. In the case of neutron counting the geometry affects the self-multiplication [6]. Recently [7] we have used our Pu samples to test the accuracy of Pu-decay corrections; in particular the possibility that decay constants depend on whether the Pu is in a conducting or insulating form. One of the major limitations was the accuracy to which the self multiplication M could be estimated from the capsule design and fill height estimate made at the time of preparation. To illustrate this point, if M exceeds unity by a small amount δ the Reals coincidence (Doubles) rate is enhanced by a factor of about $(1+5.4\delta)$ for RG PuO_2 while the Triples rate is enhanced by a factor of about $(1+17\delta)$ and so any uncertainty in δ gets amplified. In the work cited the resulting uncertainties on the two small oxide samples studied (Pu-240eff masses of 0.112 g and 0.224 g for sources AE4043/2 and AE4043/3 respectively) was ±0.16% & ±0.2% and ±0.5% & ±0.65% for Double and Triples in the two sources

respectively. These figures indicate that even well characterized, well described calibration standards with an established track record can be accuracy limiting when one drives to advance the state of the art.

In this work we explain a series of empirical investigations undertaken to better understand the PuO_2 distribution (e.g. density and fill height) in the AE4043/nn series of reference sources. The findings are used to permit improved calculations of the gamma-ray self attenuation factors and self multiplication enhancements.

AE4043/NN SOURCES

In order to correctly model the sources they must first be examined and their structure understood in detail. The AE4043/nn sources are stainless steel double encapsulated PuO_2 sources containing the relative isotopic composition in Table I. Although the outer structure of the sources are documented thoroughly [8] and a set of unused capsule components is available, the internal composition (PuO_2 density, fill height, symmetry etc.) is not well known for our present purposes.

Table I Isotopics for AE4043/nn Sources, Measured 27 January 1990 [8] and Calculated 20 January 2006

	Measured 27/01/90		Calculated 20/01/07	
Isotope	Weight %	Uncertainty %	Weight %	Uncertainty %
Pu-238	0.121	0.001	0.107	0.001
Pu-239	76.792	0.022	76.702	0.022
Pu-240	21.336	0.019	21.564	0.019
Pu-241	2.052	0.002	0.917	0.010
Pu-242	0.701	0.002	0.710	0.002
Am-241 (with respect to total Pu)	817 ppm	2 ppm	12228 ppm	103 ppm

The 1.3 mm thick stainless steel capsules are shown in Fig. 1. Fig. 2 shows the components of the stainless steel encapsulated sources, including the tools for extracting the inner plunger cup and compressing the PuO_2.

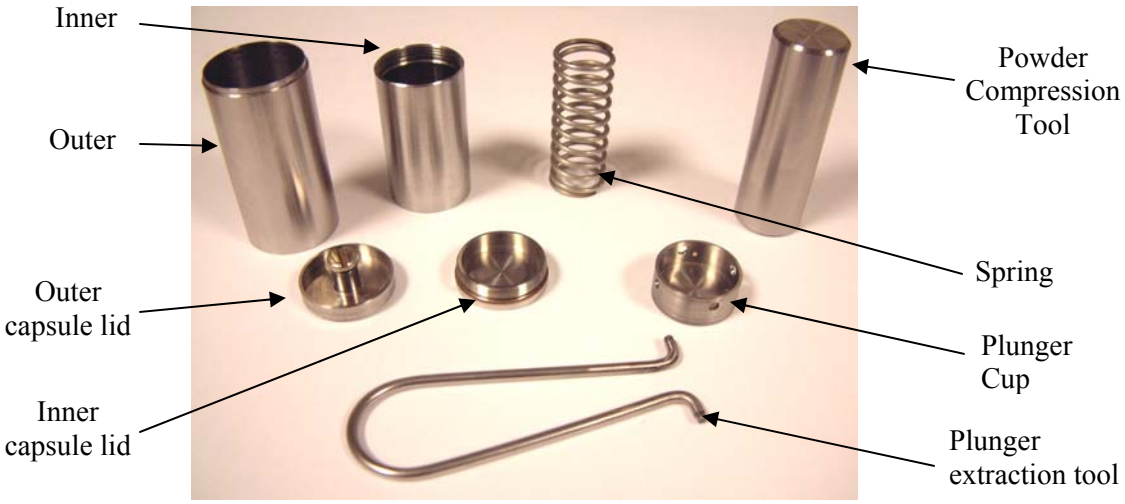

Fig. 1. The AE4043/nn source components including the inner and outer capsule and lids, plunger cup, spring, compression tool and cup extraction tool (excluding the spring locators)

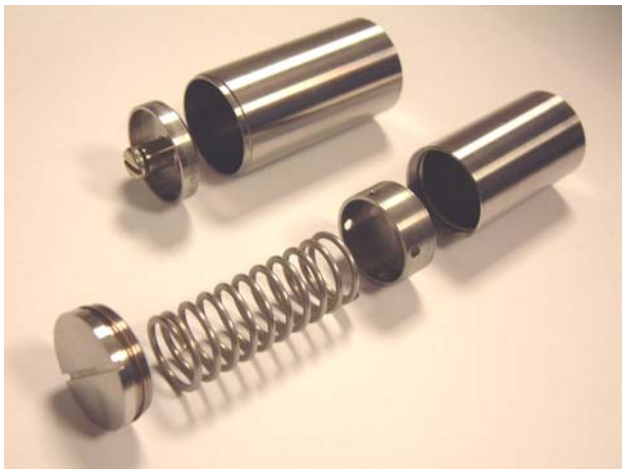

Fig. 2. The AE4043/nn source component configuration minus the spring locators

The source components are configured as shown in the photograph in Fig. 2 and the internal sketch in Fig. 3. The PuO_2 is compressed into the base of the inner capsule using the special purpose tool and the plunger cup. This is then held in place firmly by the spring and locators, which is secured between the cup and the inner capsule lid. The inner capsule is then fitted into the outer capsule and sealed. The spring was not fitted for sources containing greater than 28g of PuO_2 (items AE4043/9 and /10), there not being sufficient room.

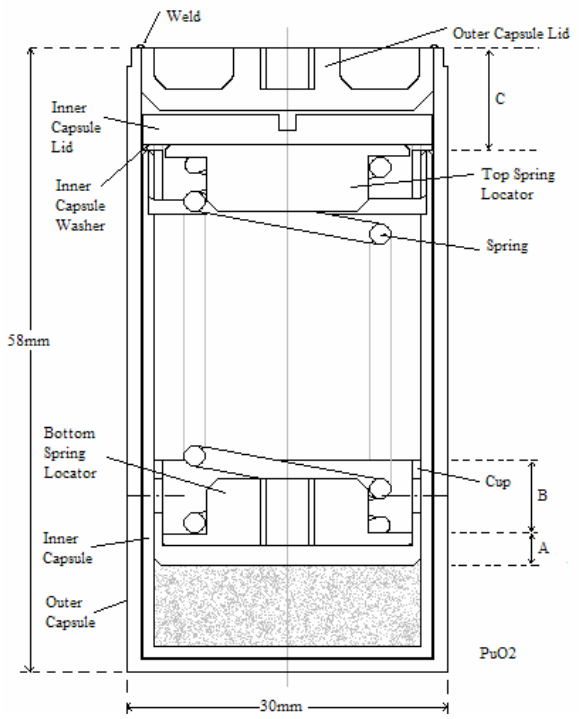

Fig. 3. The AE4043/nn source internal capsule components and basic dimensions, re-sketched from [8]

The source sizes used range from 0.099g to 24.70g of Pu (0.11g to 28.25g of PuO_2) as shown in **Table II**. This table also contains a rough estimate of the PuO_2 fill height within the inner capsule based upon a density of 1.856g.cm^{-3}; however the true density of the powder is not specified. It is determined from observations of Fig. 3

and micrometer measurements that the internal diameter of the inner capsule is accurately 25mm, the inner capsule is 1.11mm thick, the outer capsule is 1.14mm thick and the gap between the two capsules is 0.25mm.

Table II AE4043/nn Source Pu and PuO_2 Content and Calculated Fill Heights Assuming a Density of 1.856 $g.cm^{-3}$

Source ID	PuO_2 mass (g)	Pu mass (g)	Fill height (mm)
AE4043/1	0.113	0.099	0.12
AE4043/2	0.565	0.494	0.62
AE4043/3	1.128	0.986	1.24
AE4043/4	2.261	1.977	2.48
AE4043/5	5.650	4.941	6.20
AE4043/6	8.479	7.414	9.31
AE4043/7	11.298	9.879	12.40
AE4043/8	22.597	19.758	24.80
AE4043/9	28.246	24.697	31.00
AE4043/10	28.252	24.702	31.01

AE4043/NN PRELIMINARY SOURCE MEASUREMENTS

Two sets of spectroscopic measurements have been performed using a 70mm diameter by 20mm thick CANBERRA type BEGe3820 high purity germanium detector, to observe the self attenuation taking place in the AE4043/nn sources. The apparatus was constructed on a horizontal bench, as shown in Fig. 4 so that the active source material was approximately level with the center of the detector, with the relevant edge of the source casing at either 400mm or 430mm from the front face of the detector capsule. The AE4043/nn sources were measured in two different orientations: upright (as shown with the active material at the base) and horizontally (on their side with the active material nearest to the detector). The sources were separated from the detector by a 1.5mm thick Cd attenuator sheet to reduce the high count rate from the lower energy gamma rays, especially the intense 60keV radiation from ^{241}Am which grows in from the decay of ^{241}Pu.

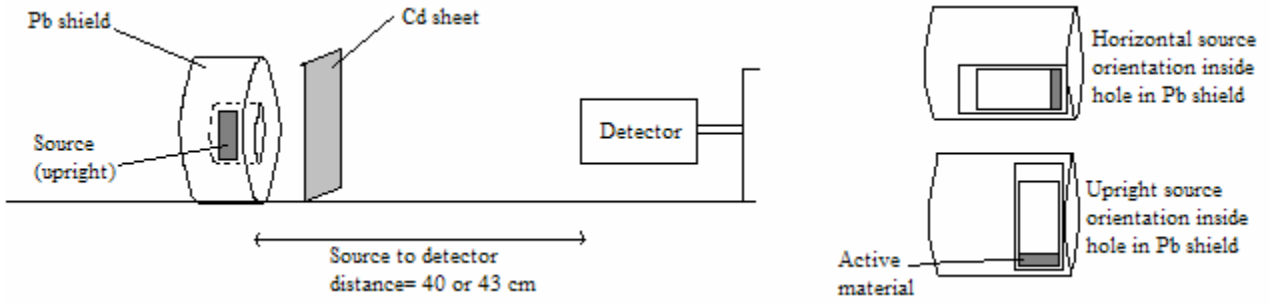

Fig. 4. AE4043/nn sources preliminary test measurements with source in the upright position

Energy and efficiency calibrations were performed with a certified multi-line (^{241}Am, ^{133}Ba, ^{137}Cs, ^{152}Eu) source and a reference pulser was used to perform the dead time correction. The 129keV and 414keV apparent mass results are plotted in Fig. 5 and Fig. 6, respectively for both measurement sets and source orientations. Also plotted are the measurement uncertainties estimated at the 1-σ level.

For the sources orientated in the upright position, with the axis of the source material normal to the detector axis, the thickness of PuO_2 seen by the detector remains constant as the mass (and fill height) increases. Consequently the apparent masses of the 129keV and 414keV lines increase linearly (allowing for statistical fluctuations) in direct proportion to the fill height assuming that the bulk density is constant for all sources. For the sources lying

horizontally with the circular base at right angles to the detector axis, the apparent mass of PuO_2 increases with source mass until the gamma-rays can no longer penetrate the PuO_2 to reach the detector. For the 129keV lines this occurs at a source mass of approximately 5g (apparent mass 0.83±0.16g). Fig. 6 demonstrates that the 414keV gamma rays also suffer from the same effect but much less strongly.

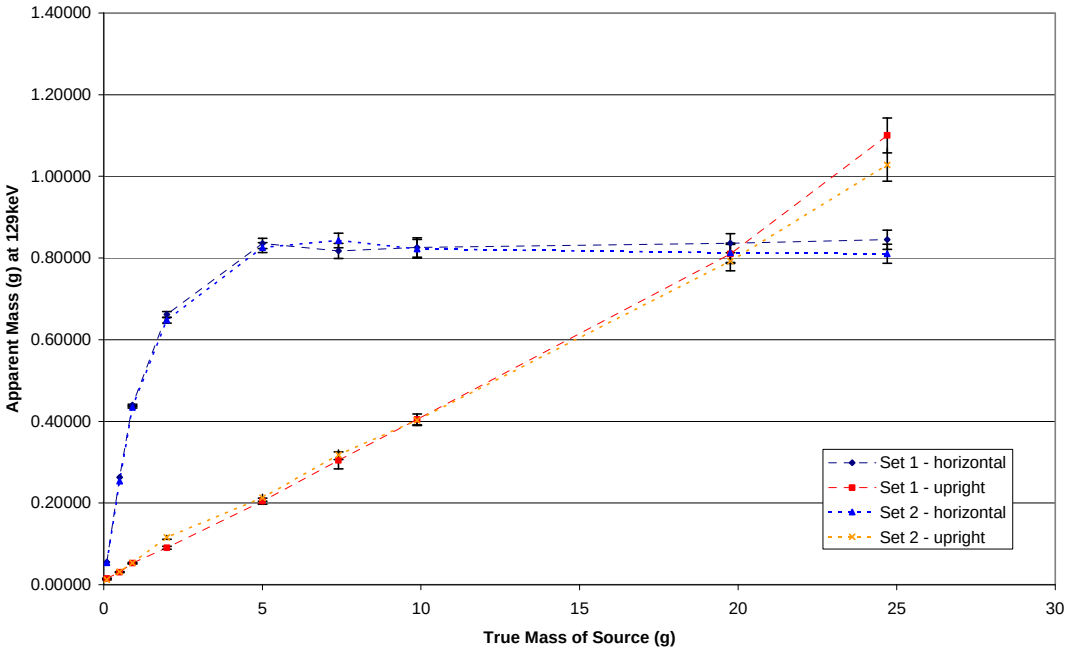

Fig. 5. Graph showing the measured apparent masses for two sets of measurements at 129keV for the AE4043/nn sources for both horizontal and upright source orientations

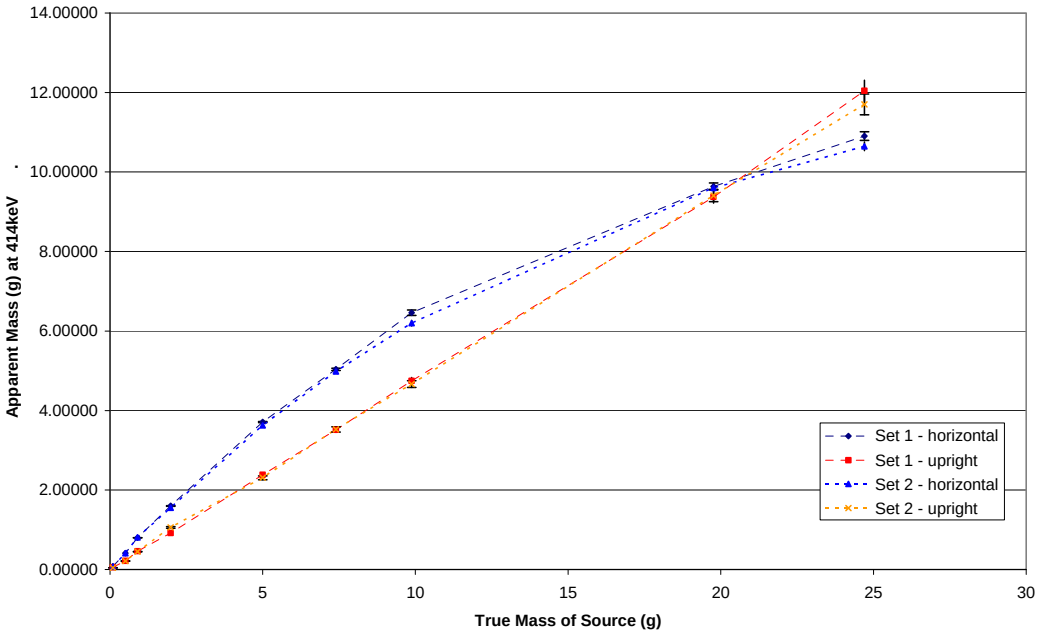

Fig. 6. Graph showing the measured apparent masses for two sets of measurements at 414keV for the AE4043/nn sources for both horizontal and upright source orientations

AE4043/NN PUO_2 DENSITY DETERMINATION

Previous studies at by Croft et al [2] adopted a density of 1.51g.cm^{-3} for all sources, estimated assuming that the PuO_2 powder in AE4043/9 and /10 fills the inner capsules since their springs are not present. These studies were later revisited [Croft, unpublished] and densities between 1.72g.cm^{-3} and 2.03g.cm^{-3} were adopted for the sources based upon plunger measurements taken at the time of fabrication and consistent with the understanding about the length of the springs which holds the plunger caps in place*.

In order to better estimate and independently confirm the density of the AE4043/nn sources the fill-height of a selection of sources must be determined from experimental data. An experiment has been set up for this purpose, as shown in Fig. 7.

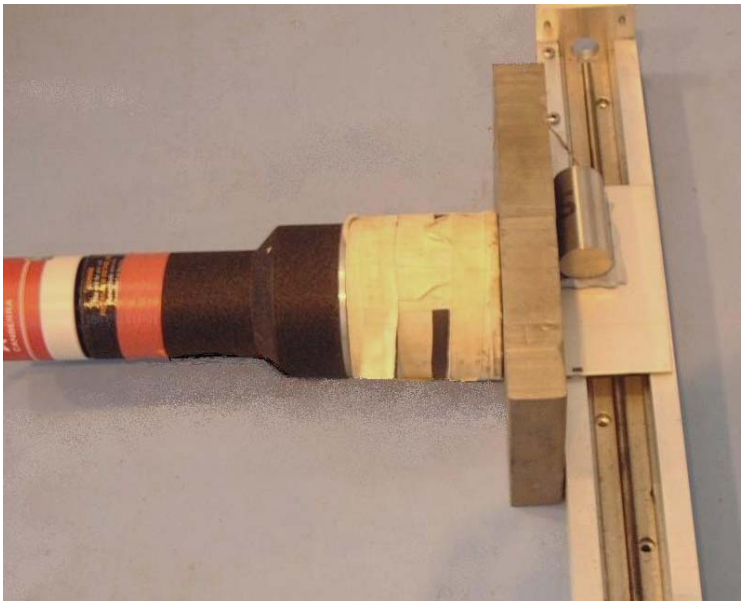

Fig. 7. Photograph of the machine slide experiment used for powder distribution and fill-height measurements of the AE4043/nn sources

The equipment consists of a 76mm diameter by 76mm long sodium iodide (NaI) detector connected to a CANBERRA UniSpec multichannel analyzer, set perpendicular to a machine slide, and separated from the source by a 30mm deep tungsten collimator with a 1mm hole. The instruments were secured to the table so that the source, detector and machine slide could not move independently (not shown in the Figure). The initial source position was beyond the view of the detector through the collimator and was moved in 0.25 to 0.5mm steps using the manually operated machine slide so that the side of the source passed along the sight of the collimator, until the measured count rate returned to its original value and remained at this level for several measurements steps.

The dead time corrected counts in the 60keV peak Region of Interest (ROI) (from ^{241}Am) were recorded for regular periods (the duration depends on source strength) using Genie^{TM} 2000 Gamma Acquisition and Analysis [9]. The 60keV peak was chosen since it has a high intensity and is at a relatively low energy and so the collimator defines the Field of View (FoV) most tightly.

---

* For information the density estimates taken across the ten source, smallest to largest, derived form the earlier unpublished review were: 1.73, 1.73, 1.64, 1.92, 1.80, 1.66, 1.72, 1.74, 2.03, 1.83 g.cm^{-3} with nominal uncertainties of roughly ±5% used for self-multiplication sensitivity studies

For the purpose of this experiment it is assumed that at the very true-edge of the active material the collimated detector will observe half of what it would observe for an infinite material because the edge of the source is exactly half way across the collimator gap. Consequently the Full Width Half Maximum (FWHM) of the spatial count rate profile should give a fair estimate of the thickness (height) of active material in the source. In order for this assumption to apply the spatial profile must also reach a definite peak region so the FWHM may be correctly calculated. Therefore the source must be of sufficient height so that a flat region is observed where the count rate is unaffected by the edges of the active material. Calculations show that the FoV of the source from the detector is approximately 1.4mm and so the measured source must have a fill height greater than this value. Consequently, this process has been performed for 6 sources: AE4043/5, 6, 7, 8, 9 and 10 (approximately 5g, 7.5g, 10g , 20g, 25g and 25g respectively) (see Table II). An example of the spatial profile for AE4043/6 is shown in Fig. 8.

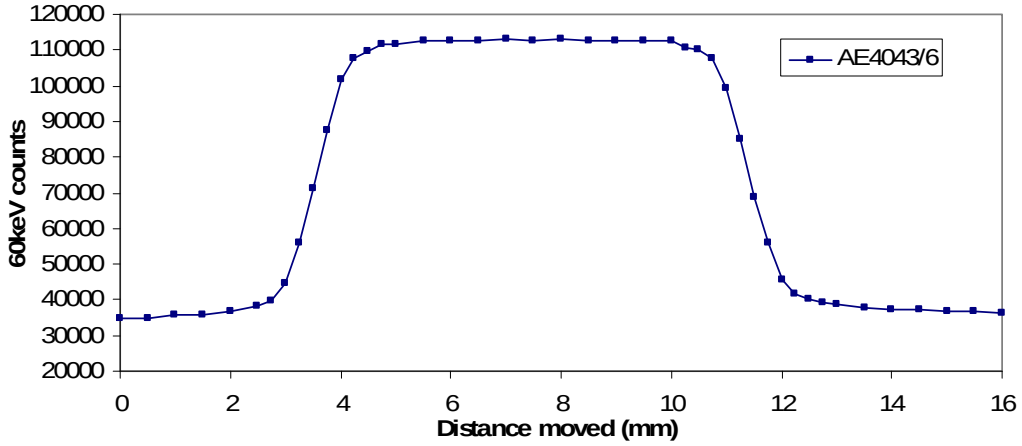

Fig. 8. Spatial profile for 60keV activity distribution in the 7.5g AE4043/6 source

To calculate the effective density of the PuO_2 in the source, the FWHM of the distribution must first be found. For this example the average background signal level was 35,500 counts, and the average peak level was 112,800 counts. Therefore the Half Maximum (HM) value is 74,150 counts (after accounting for the pedestal background) and it can then be determined between which two pairs of source locations the FWHM should be calculated. It is assumed that the graph is linear between the pair of the points and so by plotting the straight line and using the HM value as the co-ordinate the FWHM may be determined. Table III and Fig. 9 show the results for four of the six sources in the set. The remaining two sources have been omitted as explained below.

Table III AE4043/5, 6, 7 & 8 Measured FWHM and Calculated Densities Using the NaI(Tl) Scan Data

Source	FWHM = fill height (mm)	Mass of PuO_2 (g)	Calculated Density ($g.cm^{-3}$)	Uncertainty ($g.cm^{-3}$)
AE4043/5	5.390 ± 0.14	5.56	2.14	0.11
AE4043/6	7.876 ± 0.14	8.48	2.20	0.05
AE4043/7	10.310 ± 0.14	11.30	2.23	0.03
AE4043/8	21.092 ± 0.14	22.60	2.18	0.01

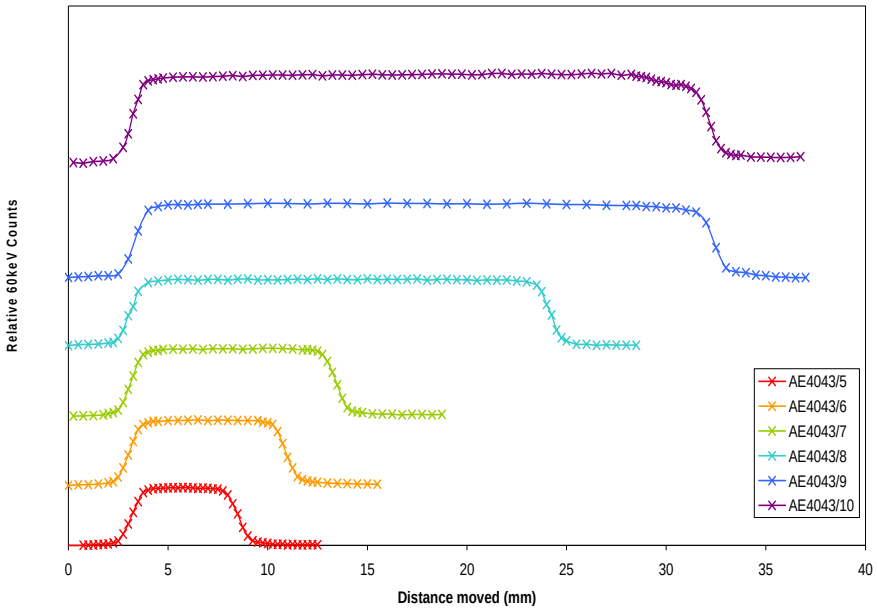

Fig. 9. Graph showing the relative 60keV counts versus the distance moved for sources AE4043/5-10

The heights of the maximum and minimum flat regions have been calculated using an average of all data points at this level and so their error is treated as negligible. Similarly, since the gradient is determined from the nearest two points, then the gradient uncertainty is neglected. The FWHM uncertainty is calculated as the quadrature sum of the statistical measurement uncertainty ($\sqrt{N}$ where N is the number of counts) and the uncertainty in the location of the machine slide (approximately 0.1mm). The uncertainty in the density is then calculated by propagating the uncertainty in the FWHM.

In some of the sources measured there is a small difference in start and end values, which may be due to the cap having a small groove along its outer edge, designed to allow air to flow out whilst it is being put in place, or may be due to loose powder residing above the cap if the inner capsule was contaminated during assembly. It should also be noted that these measurements were not background subtracted since an ROI was used to determine the 60keV counts rather than using the net peak area. Consequently the background may increase as the source is moved to a position where coherent scattering could affect the number of counts reaching the detector. Similarly if the side of the source was not completely parallel to the detector face, then the flat top of the profile may appear to rise or fall as the source is scanned. Where a difference in start and end values is observed an average of the start and end value (the background level with the collimator not viewing the source) has been used as the background signal in the density calculations.

The results indicate that the PuO_2 powder inside the capsules had an average density of ~ $(2.19\pm0.04)g.cm^{-3}$. However, it appears from the lower three results that the density is increasing with mass. This may be since the cap which holds the powder in place is held down by a cut spring. The uncompressed length of the cut springs is not documented. As the fill height increases there may more pressure from the spring and so the powder may be more compressed. However, observations of data from Fig. 6 indicate that the 414keV apparent mass behaves linearly with mass and so it is assumed that the density is approximately constant through the set of sources (radial variations are not accessible).

Observations of the spatial profile of the AE4043/10 (approximately 25g Pu) source (and AE4043/9 to a lesser extent) indicate that the internal geometry of the two largest sources is different from that of the others. Consequently, this result is not valid for the purpose of forming an average density estimation.

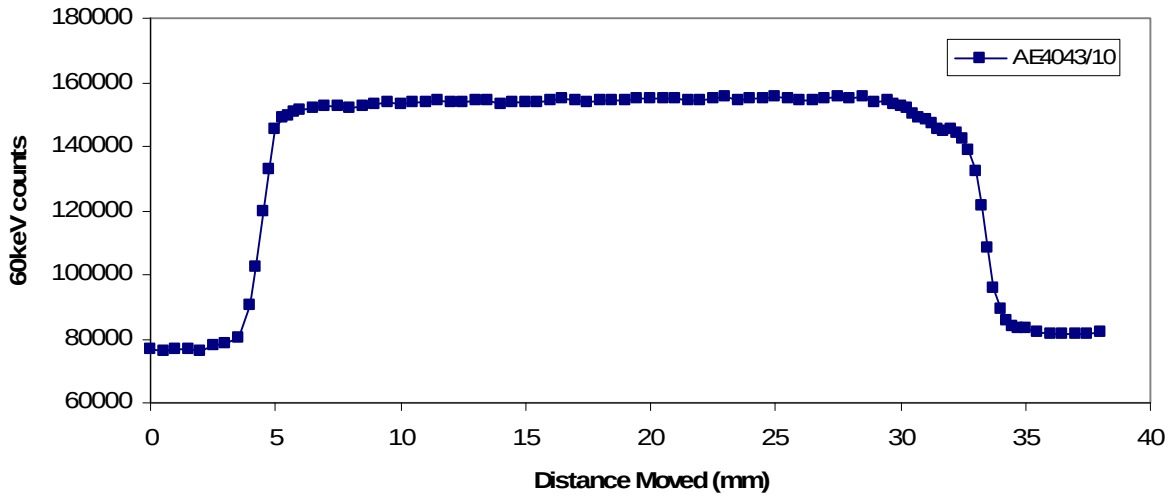

Fig. 10. Spatial profile for 60keV activity distribution in the 25g AE4043/10 source

The number of 60keV counts versus distance moved graph for AE4043/10 is shown in Fig. 10. The number of 60keV counts rises similarly to the other sources, however the descending curve behaves somewhat differently; there is an initial slower decrease in the number of counts from 30mm to 33mm and then the number of counts decreases to a value slightly higher than the initial background level. This initial decrease may be due to the fact that the higher mass sources do not contain a spring to hold the cap in place and so it is possible that the cap may have moved, allowing the PuO_2 powder to move more freely at the top of the capsule, and hence be less dense than the main body of powder.

To calculate the density of the main body of PuO_2 powder of the AE4043/10 source it has been assumed that the FWHM can be taken from the half maximum on the ascending line and the half maximum at an imaginary line drawn from where the count rate initially starts to descend. This assumption leads to an approximate density of 2.17 $g.cm^{-3}$, whereas using the plotted descending line gives an average density of 1.99 $g.cm^{-3}$. A similar analysis of the AE4043/9 source gives 2.08 $g.cm^{-3}$ and 1.98 $g.cm^{-3}$ respectively – which shows similarity between these two sources which is as expected.

AE4043/NN POWDER DISTRIBUTION MEASUREMENTS

Previous work (unpublished) of the AE4043/nn sources has shown the AE4043/1 source to measure a consistently low mass of approximately 55mg by gamma assay. The cause may be a result of an asymmetrical Pu powder distribution, or the powder may reside within a ring on the outer diameter of the inner capsule due to the small fill-height, held in place by the raised edge on the base of the plunger cup (see Fig. 3). To test this hypothesis an experimental set-up similar to that shown in Fig. 7 was used except that the source was rotated horizontally by 90^o so that the base of the source container is parallel to the flat surface of the detector. The 60keV count rate is observed across the base of the AE4043/1 in two dimensions (i.e. by rotating the source about its axis 90^o and re-measuring) and the AE4043/5 serves as a control case to observe the expected behavior for a source with uniformly distributed activity. The resulting profile for the 5g source is shown in Fig. 11 and demonstrates a symmetrical powder distribution. The profile is a dome shape since as the collimator is moved across the base of the capsule the visible chord length (y) increases as a function of the apothem (x) (or distance moved across the source) until the diameter length (R/2) is reached at the central position, and then decreases symmetrically using the equation below:

$$y = 2\sqrt{R^2 - x^2}$$

This equation has been normalized to the measured curve and plotted alongside the measured count profile in Fig. 11 to demonstrate the expected behavior of the spatial profile. The two curves match within statistical fluctuations and so the AE4043/5 source may be taken to be symmetrical with uniform PuO_2 powder distribution across the base of the capsule.

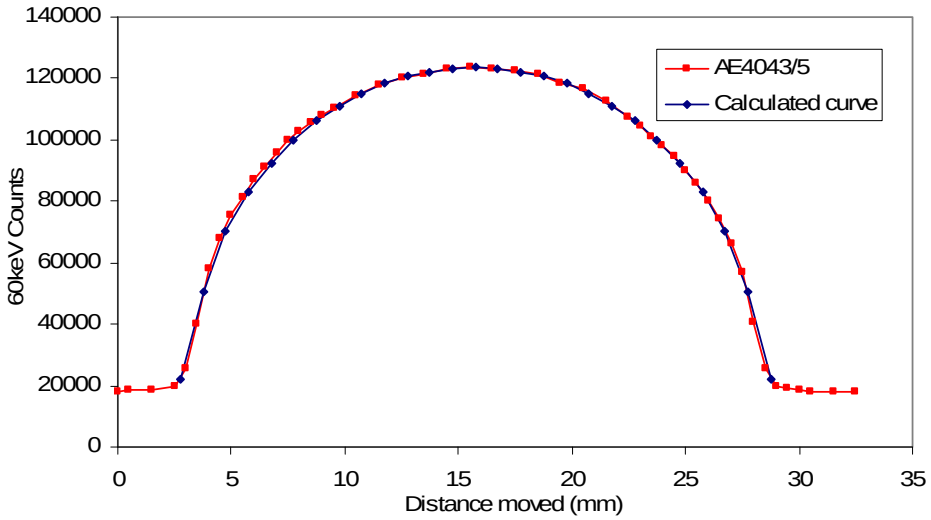

Fig. 11. The 60keV profile of AE4043/5 across the base demonstrating uniform PuO_2 powder distribution

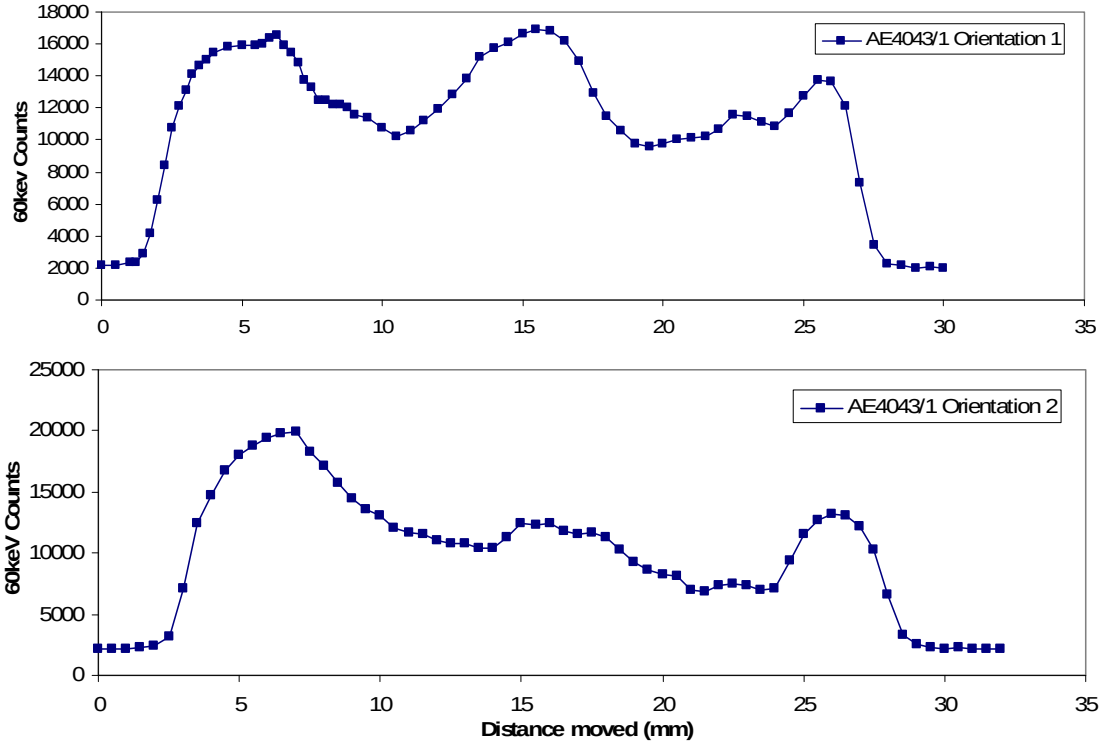

Fig. 12. The AE4043/1 source 60keV profile across the base of the source in 2 different orientations

The profile for the AE4043/1 source is shown in Fig. 12 for two different orientations with the source rotated about its axis by 90°. The number of counts for the two orientations is different in the center since the source was not at a consistent distance from the detector and collimator; however the base of the source was set parallel to the collimator and detector face in each situation. The spatial profiles show that the activity is neither symmetrical nor uniform across the base of the capsule. The active material appears to reside mostly in the rim area around the outer edge of the inner capsule, with possibly a small amount of active material remaining in the inner section.

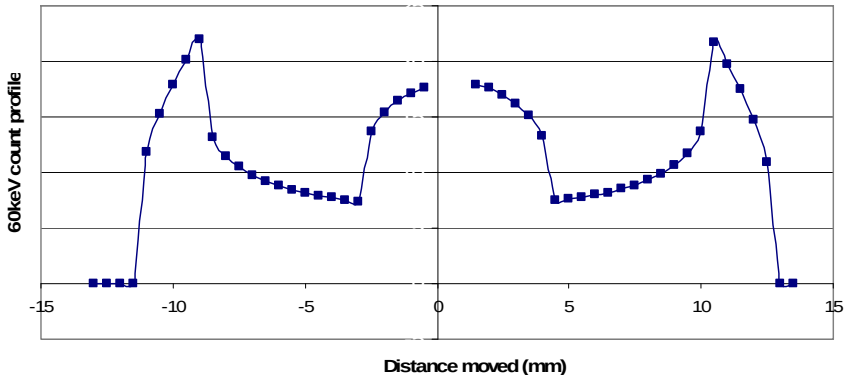

Fig. 13. Expected 60keV spatial profile for a uniformly thick source consisting of active powder in a 2.5mm thick ring around the outside plus a 4mm radius circle in the center

Fig. 13 demonstrates, as an example, the calculated spatial profile for a source consisting of a 2.5mm thick ring of active powder around the outside of the cap plus a 4mm radius circle of powder in the center (where all powder has an equal fill height). The measured profiles are far less symmetric and the powder appears to be more randomly distributed across the central section, indicating that the PuO_2 powder may be mobile below the cap within the capsule. To test this, the AE4043/1 source has been measured in the same orientation a further two times after the source has been tapped gently on the left (Fig. 14: Measurement 1) and the right (Fig. 14: Measurement 2) i.e. at 90° either side of the measured orientation.

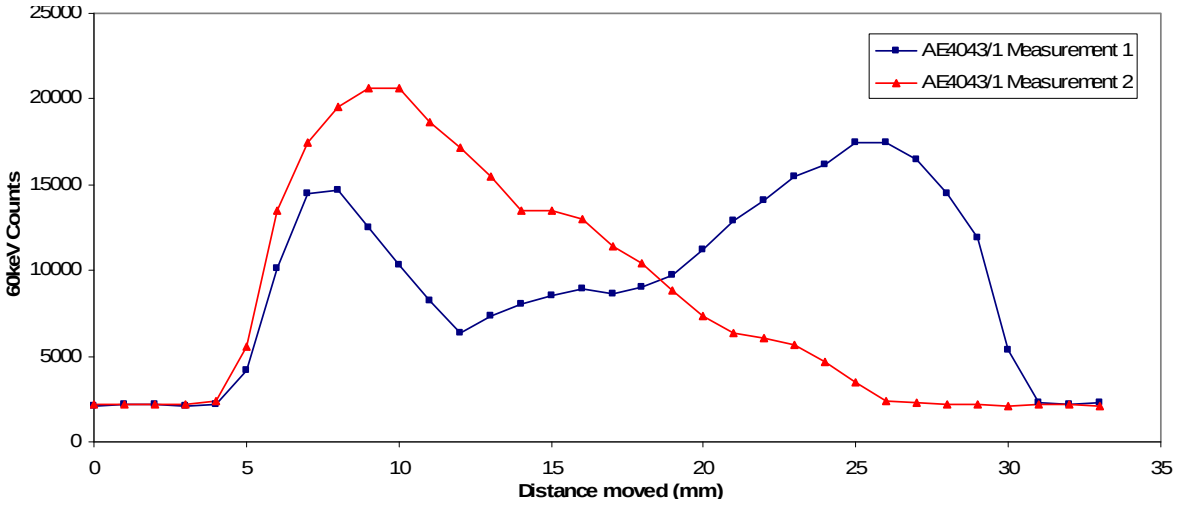

Fig. 14. AE4043/1 counts across the base of the source after gently tapping the capsule on either side

Fig. 14 shows a clear difference between the two measurements. In each case the powder appears to have moved towards the lower side after being tapped. The second "tapping" has caused the powder that once resided around the outer ring to slip to the opposite side.

AE4043 MODELING

Selected AE4043/nn sources (omitting sources AE4043/1, 9 and 10 for the reasons explained) have been modeled using the point source model to support the density and fill height measurement results in the previous section, and to assist in validating the point source model.

Table IV AE Source Pu and PuO_2 Content and Calculated Fill Heights Assuming a Density of 2.19 $g.cm^{-3}$

Source ID	PuO_2 mass (g)	Pu mass (g)	Fill height (mm)
AE4043/2	0.565	0.494	0.53
AE4043/3	1.128	0.986	1.05
AE4043/4	2.261	1.977	2.10
AE4043/5	5.650	4.941	5.26
AE4043/6	8.479	7.414	7.89
AE4043/7	11.298	9.879	10.51
AE4043/8	22.597	19.758	21.02

The PuO_2 density is assumed to be 2.19 $g.cm^{-3}$, and the material is uniformly distributed (except for sources AE4043/1, 9 and 10 - see earlier discussion). From these assumptions the thickness of the PuO_2 powder may be calculated as being in the range 0.53mm to 21mm (see Table IV).

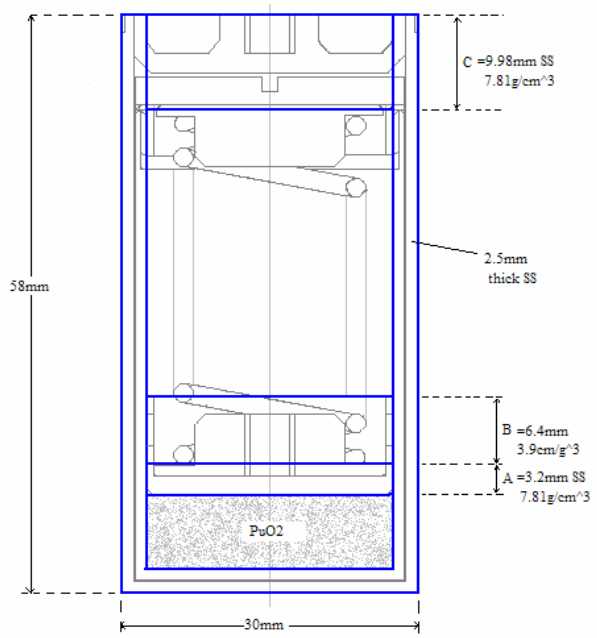

Fig. 15. AE4043/nn source showing blue lines for the modeled set-up

The stainless steel (SS) was modeled using the CANBERRA Genie 2000 ISOCS MuEditor [see 9 and navigate] program as:

- C: 0.08wt%
- Cr: 19.0wt%
- Fe: 71.92wt%
- Ni: 9.0wt%

with a density of 7.81 $g.cm^{-3}$. The AE4043/nn source was modeled as shown by the blue lines (highlighted) in Fig. 15. Areas A and C and the outer encapsulation are modeled as solid SS. Area B was modeled as SS with half the normal density, 3.905 $g.cm^{-3}$. Due to the manufacturing process of the sources all Pu powder should reside within the area below the cap in the inner capsule, and the powder should be distributed symmetrically within this area. The sources were modeled with this distribution, with the fill heights stated in Table IV.

The BEGe detector was modeled as a 70mm diameter, 21mm thick uncollimated Ge crystal at 400mm from the source, to mirror the experimental set-up. The ratio of attenuated to unattenuated counts were recorded for the 129keV and 414keV lines for the 7 selected sources.

Preliminary results show that for both lines the modeled results are larger than the measured results. However, there are a number of factors which could bias the measured and modeled results. For example the measured results depend on the accuracy of techniques such as the efficiency and dead time corrections, and nuclide library parameters such as the branching ratio of the lines. If these are not accurate then the modeled and measured results will differ. The modeled results also may be affected by encapsulation assumptions, the estimated average density or the value of the mass attenuation coefficient (μ) used. These preliminary results use a value of μ as set by CANBERRA's Genie ISOCS which excludes coherent scattering (coherent scattering redirects the photon without energy loss and to a first approximation in scatter and out scatter compensate). The modeling was repeated with values of μ taken from the XCOM database [10] both with and without coherent scattering (see Fig. 16). We note that evaluated reference data from different sources varies since the selection of data and methods of evaluation differ. Variations are therefore in some sense indicative of our current state of knowledge.

As seen in the plots, for all sets of results the measured values appear to "dip" for the 5g source relative to those calculated. This may be due to an anomaly in the measured dataset. Also the smaller sources appear to have a lower measured to modeled ratio; this may be a consequence of a non-uniform density across the set of sources.

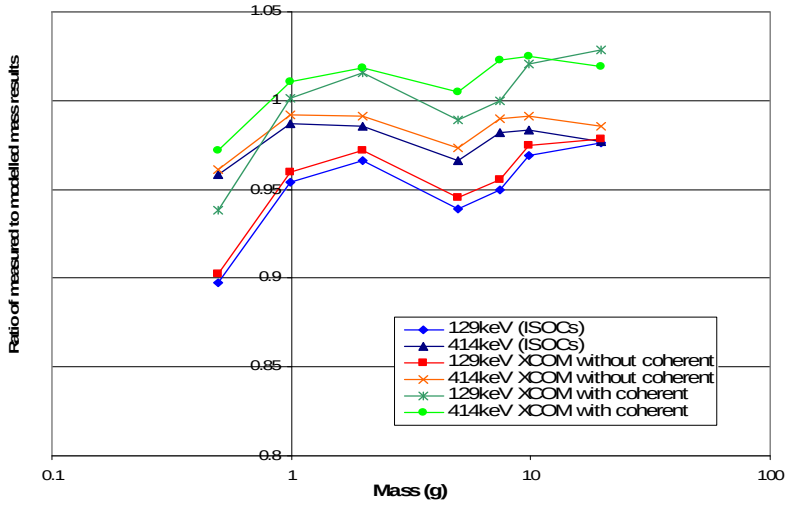

Fig. 16. Graph showing the measured to modelled mass ratio for selected AE4043/nn sources for the 129keV and 414eV lines for different choices of interaction coefficients

Although the results show better agreement when the μ-values are taken from XCOM without coherent scattering when compared to those using the original Genie ISOCs μ-values, the modelling calculations still produce results that are too large. In contrast, the results obtained using the XCOM with coherent scattering μ values are on average slightly too small. This is because, if the μ value includes coherent scattering, the attenuation coefficient (and collision cross-section) is larger and so the apparent mass calculated by the model is smaller.

Physically the apparent μ (the μ that should be used in the model to produce the result that one would obtain with all the scattering in the real sample) may lie somewhere between the two values since the μ values do not account for situations where the gamma ray is initially not directed towards the detector but is coherently scattered towards it. It would be possible to determine the 'true' μ-value by modeling the geometrical set-up of the experiment, including surrounding objects and equipment, using complex simulation tools; however this has not been performed since the benefit of the results would not be significant for the purposes of this report.

PU SELF-ABSORPTION CORRECTION

In earlier work we have re-examined how an experimental plutonium self absorption correction (SAC) may be derived based on the observed apparent masses as a function of line energy. A mathematical approach was adopted where the nature of the study involved calculating the behavior of a large range of lump types (shapes, compounds and densities) and letting the model reveal the correlations with promise [4, 5]. The results of these calculations have been fitted to a numerical SAC algorithm which has been developed into a functional self-absorption engine for Pu.

The correction method has been applied to lumps that are of simple shapes and uniform density and is based on the use of a single pair of γ-ray lines. In practice the majority of waste items will contain multiple lumps with a distribution of lump shapes and sizes. This effect has been studied and the method has been found to perform well across the range.

It is recognized that implementation of a SAC in practice is a challenging undertaking. No method can be viewed as perfect and one must have realistic expectations. One expression of this is in the uncertainty estimate assigned to the corrected mass. This must include the appropriateness of the underlying model for the unknown situation at hand. The lump correction must also be robust and quantified against imperfections in the gross matrix correction factors applied such as may be introduced by localized shielding effects and the spatial distribution of Pu. The latter situation could arise if a lump of fissile material had been pre-packaged before being placed into the disposal drum. These effects may be investigated by performing experimental measurements using the stainless steel encapsulated sources described above in controlled experiments. The measurements described here allow the physical sources available (which are encapsulated and in some cases optically thick) to be corrected and used in such studies.

CONCLUSIONS

The AE4043/nn Pu reference sources have been investigated and the fill-heights, density and internal arrangement have been revisited. Measurement results indicate that the PuO_2 powder inside the capsules is approximately constant and has an average density of $(2.19\pm0.04)g.cm^{-3}$. Observations of the spatial profile of sources AE4043/1, AE4043/9 and AE4043/10 indicate that the PuO_2 is mobile within the capsule. This limits the accuracy to which gamma and neutron correction factors can be made. In use, the sources must be handled with care in a consistent manner and tapped into place to settle the powder. For waste and many other practical applications the uncertainties in the correction factors are relatively minor. However as instrument performance improves and calculational tools advance continuous improvement in the experimental methods must also be made.

REFERENCES

1. S CROFT and L C-A BOURVA, “Calculation of the correction factors to be applied to plutonium reference standards when used to calibrate passive neutron counters”, Proc. 23rd Annual Meeting ESARDA Symposium on Safeguards and Nuclear Material Management, Bruges, Belgium, 8-10 May 2001, EUR 19944 EN (2001).
2. S CROFT and P M J CHARD, “Neutronic characterization of plutonium oxide reference samples at Harwel”, Proc. 15th Annual ESARDA Symposium on Safeguards and Nuclear Material Management”, Vatican City, Rome, Italy, May 11-13 1993, ESARDA 26 EUR 15214 EN (1993).
3. S. CROFT, D. CURTIS, M. WORMALD, “The Calculation of Self Attenuation Factors for Simple Bodies in the Far Field Approximation”, Proc. 46th Annual Meeting of the INMM Nuclear Materials Management, Phoenix, Arizona, July 10-14 2005 (2005).
4. D. CURTIS, M. WORMALD, S. CROFT, “A Numerical Approach to Pu Gamma-Ray Self-Absorption Correction”, Proc. ICEM’05, Glasgow, UK (2005).
5. D. CURTIS, M. WORMALD, S. CROFT, “Effects of Lump Characteristics on Plutonium Self-Absorption Correction Methods”, Proc. ICEM’07, Bruges, Belgium (2007).
6. L C-A BOURVA and S CROFT, “Calculation of the neutron leakage self-multiplication for small cylindrical plutonium and mixed oxide samples”, Proc. 21st Annual ESARDA) Symposium on Safeguards and Nuclear Material Management, Seville, Spain, 4-6 May 1999, ESARDA 29 EUR 18963 EN(1999).

7. S. CROFT, R.D. McELROY, E. ALVAREZ and D. BRACKEN, "The Non Destructive Assay of Special Nuclear Materials in Different Physical Forms", Proc. 48th INMM Annual Meeting, Tucson, AZ, July 8-12 2007 (2007).
8. D. CROSSLEY, A. FUDGE, J. PECKETT, R. WILTSHIRE, A. WOOD, "The Preparation and Characterisation of Plutonium Oxide Reference Material for Non Destructive Analysis", AEA Technology AEA-FS-00374(H) (1991).
9. http://www.canberra.com/products/835.asp Genie™ 2000 Gamma Analysis Software, Canberra website. Last accessed: 10/08/06.
10. M. BERGER et al, "XCOM: Photon Cross Sections Database", National Institute of Standards and Technology website: http://physics.nist.gov/PhysRefData/Xcom/Text/XCOM.html Last accessed: 10/01/06.